Synthesis, crystal structure and Hirshfeld surface analysis of bromidotetrakis[5-(prop-2-en-1-ylsulfanyl)-1,3,4-thiadiazol-2-amine-κN^3]copper(II) bromide

**Aziz Atashov,**[a] **Mukhlisakhon Azamova,**[a] **Daminbek Ziyatov,**[a] **Zamira Uzakbergenova,**[b] **Batirbay Torambetov,**[a]* **Tamas Holczbauer,**[c] **Jamshid Ashurov**[d] **and Shakhnoza Kadirova**[a]

[a]National University of Uzbekistan named after Mirzo Ulugbek, 4 University St., Tashkent, 100174, Uzbekistan, [b]Karakalpak State University, 1 Ch. Abdirov St. Nukus, 230112, Uzbekistan, [c]Institute of Organic Chemistry, Research Centre for Natural Sciences, 2 Magyar Tudosok Korutja, H-1117 Budapest, Hungary, and [d]Institute of Bioorganic Chemistry, Academy of Sciences of Uzbekistan, M. Ulugbek, St, 83, Tashkent, 100125, Uzbekistan. *Correspondence e-mail: torambetov_b@mail.ru

A novel cationic complex, bromidotetrakis[5-(prop-2-en-1-ylsulfanyl)-1,3,4-thiadiazol-2-amine-κN^3]copper(II) bromide, [CuBr]($C_5H_7N_3S_2$)$_4$Br, was synthesized. The complex crystallizes with fourfold molecular symmetry in the tetragonal space group $P4/n$. The Cu^{II} atom exhibits a square-pyramidal coordination geometry. The Cu atom is located centrally within the complex, being coordinated by four nitrogen atoms from four AAT molecules, while a bromine anion is located at the apex of the pyramid. The amino H atoms of AAT interact with bromine from the inner and outer spheres, forming a two-dimensional network in the [100] and [010] directions. Hirshfeld surface analysis reveals that 33.7% of the intermolecular interactions are from H···H contacts, 21.2% are from S···H/H···S contacts, 13.4% are from S···S contacts and 11.0% are from C···H/H···C, while other contributions are from Br···H/H···Br and N···H/H···N contacts.

1. Chemical context

Nitrogen-containing heterocycles are a promising class of ligands for the synthesis of transition-metal complexes that are strongly responsive to the changes in external conditions (Lavrenova *et al.*, 2023). Derivatives of 1,3,4-thiadiazole represent a relatively new class of compounds that demonstrate a broad array of biological activities, making them of significant interest to various fields in medicinal chemistry and pharmacology worldwide (Gowramma *et al.*, 2018; Kaviarasan *et al.*, 2020; Upadhyay & Mishra, 2017; Yusuf *et al.*, 2008). 1,3,4-Thiadiazole derivatives exhibit many biological properties, such as antimicrobial (Li *et al.*, 2014; Chen *et al.*, 2019), antituberculosis (Foroumadi *et al.*, 2004; Kolavi *et al.*, 2006), antioxidant (Jakovljević *et al.*, 2017; Swapna *et al.*, 2013), anticancer (Altıntop *et al.*, 2018; Aliabadi, 2016), herbicidal (Wang *et al.*, 2011) and antifungal (Chen *et al.*, 2007; Karaburun *et al.*, 2018) activities. In addition, a limited number of studies mention the utilization of diverse thiadiazoles as ligands in the synthesis of biologically active metal complexes (Huxel *et al.*, 2015; Chandra *et al.*, 2015; Hangan *et al.*, 2015).

The strong complexing capability of thiadiazole derivatives is associated with the existence of numerous sulfur and nitrogen atoms and the distinctiveness of its structure, specifically, the presence of unshared electron pairs and donor
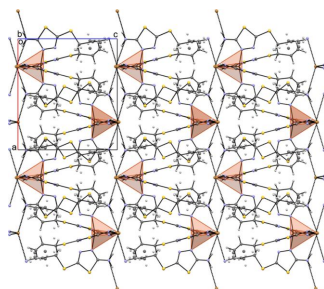
characteristics. They generate complexes with elements whose ions possess partially vacant *d*-orbitals or occupied *d*-orbitals and a low positive charge, exhibiting various polyhedral structures. In this context, investigating the complex-forming properties of thiadiazole derivatives is pertinent in delineating the characteristics of the molecular and electronic structure of the original ligands and the stereochemistry of the coordination polyhedron (Hassan *et al.*, 2018). This study focuses on the synthesis, examination of the structure, and characteristics of the [Cu(*L*)4Br]Br complex, where *L* is 2-amino-5-allylthio-1,3,4-thiadiazole (AAT), employing single-crystal X-ray diffraction (SC-XRD).
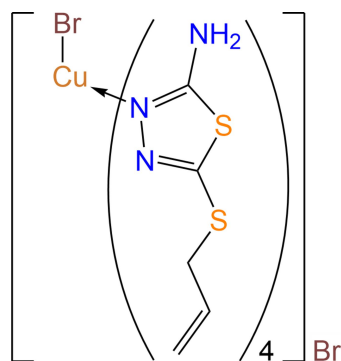
2. Structural commentary

The crystals of [Cu(AAT)$_4$Br]Br possess an ionic-molecular structure. The complex crystallizes in the fourfold tetragonal system, space group *P*4/*n*, and the asymmetric unit comprises one molecule of 2-amino-5-allylthio-1,3,4-thiadiazole (AAT), one Cu^{2+} ion with a multiplicity of 0.25, and Br$^-$ ions in two positions with multiplicities of 0.25 each. The Br$^-$ ions occupy special positions on fourfold axes, and this symmetry transformation generates the formula unit. In [Cu(AAT)$_4$Br]Br, the copper atom exhibits a square-pyramidal geometry and its coordination sphere includes four nitrogen atoms (N2) from the heterocyclic ligands and a bromine anion at the top of the pyramid. These nitrogen atoms lie in one plane. The planar AAT molecules are nearly perpendicular to this plane, exhibiting a slight twist of the Br1CuN2 planes. All the amino groups are in a *syn* arrangement. One of the Br$^-$ ions is integrated into the inner coordination sphere, while the second Br- ion resides in the outer sphere (Fig. 1). As a result, the inner coordination sphere of the complex takes the shape of a tetragonal pyramid, where the basal positions are filled by nitrogen atoms from the 2-amino-5-allylthio-1,3,4-thiadiazole ligands, and the apical position is occupied by the Br$^-$ ion.

The Cu—Br bond length in the compound measures 2.7474 (7) Å, closely resembling the Cu—Br distance in the [Cu*L*$_4$Br$_2$](H$_2$O)$_2$ molecule, which is 2.9383 Å (Berezin *et al.*, 2018). Apparently, the binding of the Br$^-$ ion into the inner coordination sphere induces a distortion of the CuN$_4$ plane. The effect of this distortion is to the reduce N—Cu—N coordination angles [88.446 (18) and 161.04 (11)°], in contrast to the angles of 90 and 180° expected in an ideal square-planar

Table 1
Hydrogen-bond geometry (Å, °).

D—H$\cdots A$	D—H	H$\cdots A$	$D\cdots A$	D—H$\cdots A$
N3—H3*A*$\cdots$Br1	0.86	2.52	3.3265 (1)	157
N3—H3*B*$\cdots$Br2	0.86	2.54	3.3685 (1)	162
C5*A*—H5*AA*$\cdots$Br1^i	0.93	3.03	3.95 (2)	175

Symmetry code: (i) $x, y, z - 1$.

structure. The sum of bond angles at the Cu atom is 353.8°. The Cu atom deviates from the (N2)$_4$ plane toward Br$^-$ by 0.333 Å. The length of the Cu—N coordination bonds is 2.0206 (17) Å, similar to those bonds in analogous complexes. For instance, in nitrato-tetrakis(2-amino-5-ethyl-1,3,4-thiadiazole)copper(II) nitrate, the average Cu—N bond length is 2.003 Å (Kadirova *et al.*, 2008), aligning with the sum of the covalent radii of Cu and N.

Additionally, the Br1 atom participates in the formation of an intramolecular hydrogen bond with hydrogen atoms of four amino groups NH$_2$ simultaneously (Table 1). By comparing the structures of some complexes based on 2-amino-1,3,4-thiadiazole derivatives, we see that copper(II) bromide, in contrast to chlorides and acetates of cobalt(II) and zinc(II) (Camí *et al.*, 2005; Song *et al.*, 2012; Wang *et al.*, 2009; Kadirova *et al.*, 2008; Ishankhodzhaeva *et al.*, 2000, 2001), exhibits a distinct behavior when reacted with 2-amino-5-allylthio-1,3,4-thiadiazole under identical conditions. Instead of forming a tetrahedral molecular complex as might be anticipated from
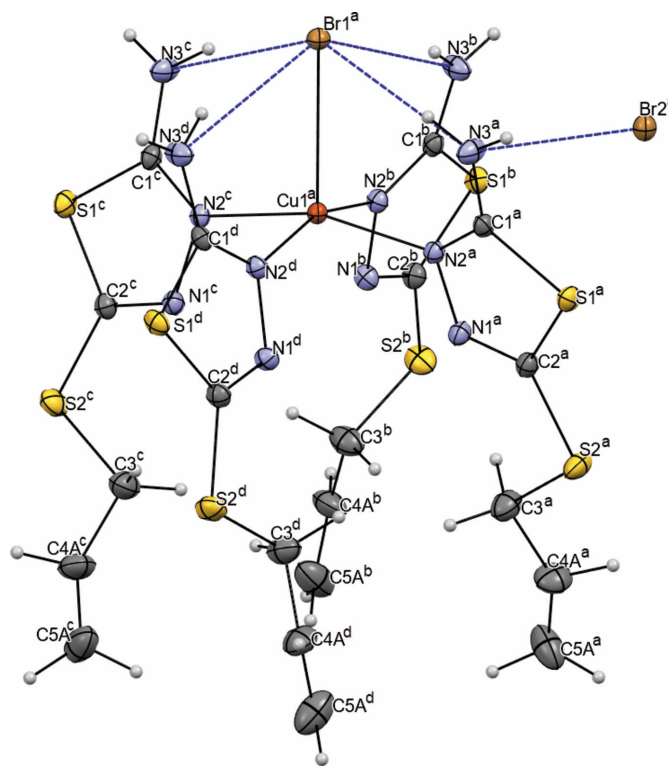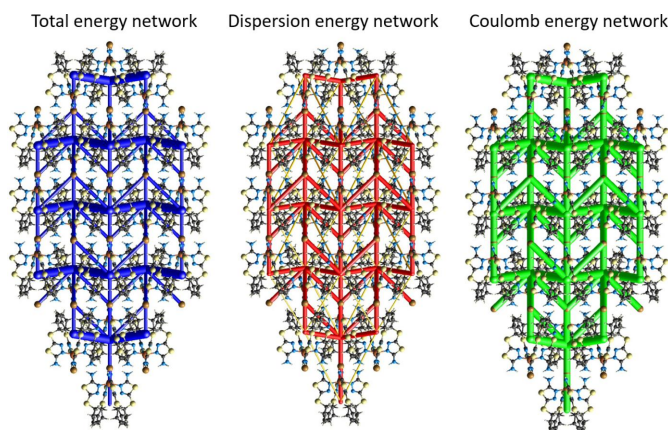

Figure 1
Molecular structure of the complex [Cu(AAT)$_4$Br]Br. Displacement ellipsoids are shown with 20% probability level for clarity. Symmetry codes: (a) $-x, y, z$; (b) $-\frac{3}{2} - y, x, z$; (c) $-\frac{3}{2} - x, \frac{3}{2} - y, z$; (d) $-y, \frac{3}{2} - x, z$.

analytical data, copper(II) bromide forms the tetragonal–pyramidal cationic complex [Cu(AAT)$_4$Br]Br.

3. Supramolecular features

In the crystal structure of [Cu(AAT)$_4$Br]Br, in addition to the aforementioned intramolecular hydrogen bonds, there exist intermolecular hydrogen bonds. The second bromide ion, positioned in the outer sphere, forms a hydrogen bond with the second (not participating in the intramolecular hydrogen bond) hydrogen atom of the amino group N3H2 (Table 1). The outer-sphere Br2 ion also resides on the fourfold axis, resulting in the generation of a layer in the crystal perpendicular to the fourfold axis due to this symmetry transformation. As a result, in the crystal packing, the cationic coordination complexes form columns along the [001] crystallographic axis (Fig. 2). The bromine anions of the outer sphere of the complex are located between the columns due to the formation of the N3—H3B···Br2 intermolecular hydrogen bonds with the amino groups of the ligand (Table 1).

The interaction energies of the secondary interactions system within the structure were calculated using the HF method (HF/3-21G) in *CrystalExplorer17* (Spackman *et al.*, 2021). Although these calculations may not yield precise values for an ionic interaction, they effectively highlight the direction of strong interactions. The result shows the total energy (E_{tot}), which is the sum of the Coulombic (E_{ele}), polar (E_{pol}), dispersion (E_{dis}) and repulsive (E_{rep}) contributions. The four energy components were scaled in the total energy (E_{tot} = 1.019E_{ele} + 0651E_{pol} + 0901E_{dis} + 0.811E_{rep}). The interaction energies were investigated for a 3.8 Å cluster around the reference molecule. The calculation reveals two stronger interactions within the neighbouring molecules. The strongest interaction total energy (E_{tot}) is −112.5 kJ mol^{-1} (∼-27 kcal mol^{-1}), with the polar (−30.1 kJ mol^{-1}), disper-
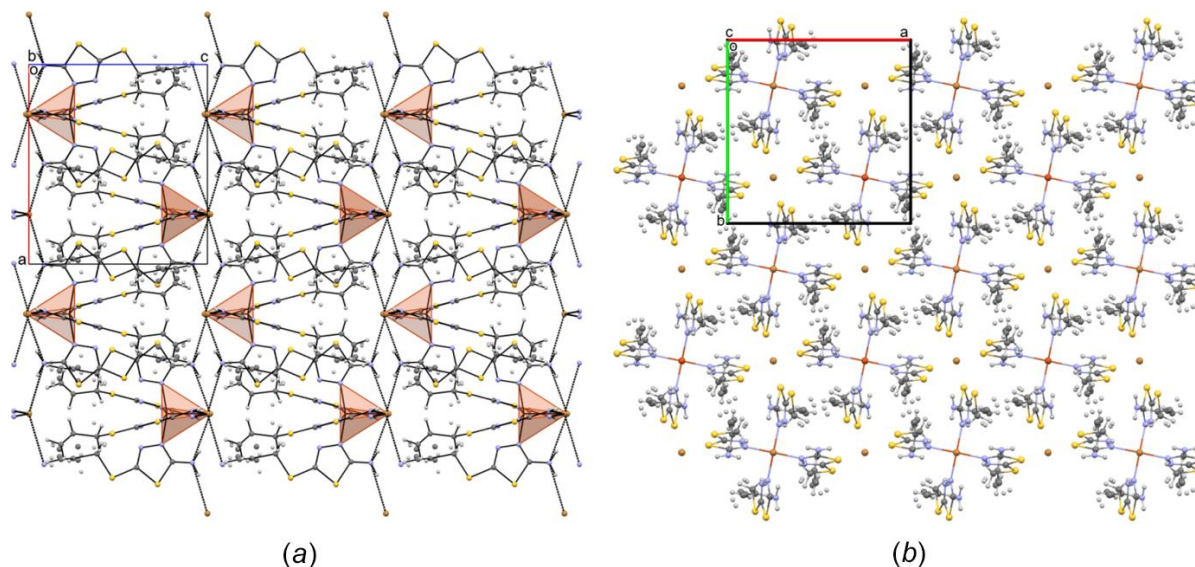

Figure 3
Interaction energy calculations within the structure were performed using the HF method (HF/3–21 G) (*CrystalExplorer17*; Spackman *et al.*, 2021. The thickness of the tube represents the value of the energy. The distribution of the interactions according to type shows strong interactions along the crystallographic *a*-axis direction (the largest values are represented here). The total energy framework (in blue) and its two main components, dispersion (in green) and Coulombic energy (in red), are shown for a cluster around a reference molecule also exhibit stronger interactions along the crystallographic *a*-axis direction.

sion (−123.3 kJ mol^{-1}), Coulombic (−58.5 kJ mol^{-1}) and repulsive (96.0 kJ mol^{-1}) energies (with green colour) (Fig. 3).

4. Hirshfeld surface analysis

To further investigate the intermolecular interactions present in the title compound, a Hirshfeld surface analysis was performed, and the two-dimensional (2D) fingerprint plots were generated with *CrystalExplorer17* (Spackman *et al.*, 2021). Fig. 4 shows the three-dimensional (3D) Hirshfeld surfaces of the complex with d_{norm} (normalized contact

Figure 2
Packing of [Cu(AAT)$_4$Br]Br complex molecules in the crystal structure in projections along the (*a*) *b* and (*b*) *c* crystallographic axis. Hydrogen bonds are indicated by blue dashed lines.
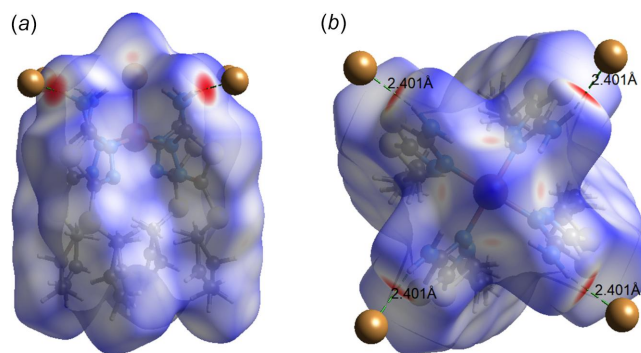
Figure 4
Views of the three-dimensional Hirshfeld surface of the complex [Cu(AAT)$_4$Br]$^+$ cation plotted over d_{norm} in views along the (*a*) [110] and (*b*) [001] directions.

distance) plotted. The hydrogen-bond interactions given in Table 1 play a key role in the molecular packing of the complex. The overall 2D fingerprint plot and those delineated into H···H, S···H/H···S, S···S, C···H/H···C, Br···H/H···Br and N···H/H···N interactions are shown in Fig. 5. The percentage contributions to the Hirshfeld surfaces from the various interatomic contacts are as follows: H···H 33.7%, S···H/H···S 21.2%, S···S 13.4, C···H/H···C 11%, Br···H/ H···Br 9.2% and N···H/H···N 7.8%. Other minor contributions to the Hirshfeld surface are: S···C/C···S 1.9% and Br···S/S···Br 1.6%.

5. Database survey

A survey of the Cambridge Structural Database (CSD, version 5.43, update of March 2022; Groom *et al.*, 2016) revealed that nearly a hundred crystal structures had been reported for complexes of 2-amino-1,3,4-thiadiazole derivatives and a number of metal ions, including Mn, Fe, Co, Ni, Cu, Zn, Mo, Ag, Pd, Cd, Sn, Re, Pt, Au and Hg, twelve of which are for Cu complexes. Six structures exhibit tetragonal–pyramidal polyhedra (HONDOG, Torambetov *et al.*, 2019; RUFQIT, Kadirova *et al.*, 2008; SUZVOY, SUZVUE, Lynch & Ewington, 2001; XIGWIU, Camí *et al.*, 2005; ZEKWOE, Gurbanov, *et al.*, 2018). In seven structures, AAT is attached to metal ions, making *p*-complexes (ODAPOC, Slyvka *et al.*,
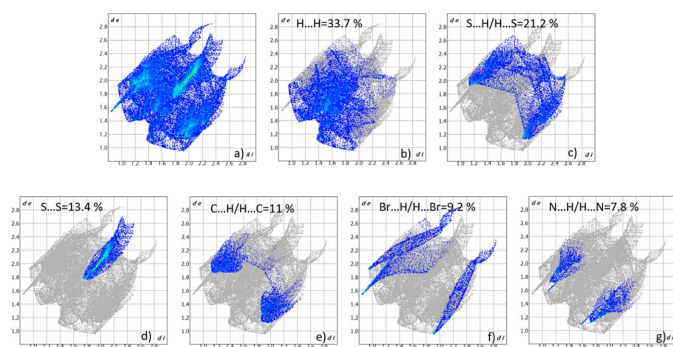
Figure 5
Contributions of the various contacts to the two-dimensional fingerprint plots built using the Hirshfeld surfaces of the title complex.

Table 2
Experimental details.

Crystal data	
Chemical formula	[CuBr(C$_5$H$_7$N$_3$S$_2$)$_4$]Br
M_r	916.38
Crystal system, space group	Tetragonal, *P*4/*n*
Temperature (K)	293
a, *c* (Å)	12.69368 (9), 11.35879 (13)
V (Å^3)	1830.24 (3)
Z	2
Radiation type	Cu *K*α
μ (mm^{-1})	7.95
Crystal size (mm)	0.12 × 0.08 × 0.03
Data collection	
Diffractometer	XtaLAB Synergy, Single source at home/near, HyPix3000
Absorption correction	Multi-scan (*CrysAlis PRO*; Rigaku OD, 2020)
T_{min}, T_{max}	0.626, 1.000
No. of measured, independent and observed [$I > 2\sigma(I)$] reflections	18450, 1746, 1597
R_{int}	0.036
$(\sin\theta/\lambda)_{max}$ (Å^{-1})	0.609
Refinement	
$R[F^2 > 2\sigma(F^2)]$, $wR(F^2)$, S	0.025, 0.065, 1.05
No. of reflections	1746
No. of parameters	118
H-atom treatment	H-atom parameters constrained
$\Delta\rho_{max}$, $\Delta\rho_{min}$ (e Å^{-3})	0.26, −0.28

Computer programs: *CrysAlis PRO* (Rigaku OD, 2020), *SHELXT* (Sheldrick, 2015*a*), *SHELXL2018/3* (Sheldrick, 2015*b*), *OLEX2* (Dolomanov *et al.*, 2009).

2022; CEDSEM, Slyvka, 2017*a*; ESIBUG, Slyvka *et al.*, 2021; HAJLUC, Ardan *et al.*, 2017; HAJMAJ, HAJMIR, Ardan *et al.*, 2017; YEBNAX, Slyvka, 2017*b*). However, no complexes of CuBr$_2$ based on 2-amino-1,3,4-thiadiazole derivatives have been documented in the CSD.

6. Synthesis and crystallization

The ligand 2-amino-5-allylthio-1,3,4-thiadiazole (AAT) was synthesized by the method of Toshmurodov *et al.* (2016), yield: 93%, m.p. = 388–390 K. CuBr$_2$·4H$_2$O (0.296g, 1 mmol) was added under continuous stirring to a solution of AAT (0.692 g, 4 mmol) dissolved in 10 ml of methanol. The resulting dark-green solution was stirred for 3 h and was then left to stand at room temperature. After one week, green crystals suitable for X-ray diffraction were obtained (yield 86%) by the slow evaporation of the solvent, m.p. = 458–460 K.

7. Refinement

Crystal data, data collection and structure refinement details are summarized in Table 2. H atoms were positioned geometrically (N—H = 0.86 Å, C—H = 0.83–0.97 Å) and refined as riding with U_{iso}(H) = 1.2U_{eq}(C, N).

References

Aliabadi, A. (2016). *Anticancer Agents Med. Chem.* **16**, 1301–1314.

Altıntop, M. D., Sever, B., Özdemir, A., Ilgın, S., Atlı, Ö., Turan-Zitouni, G. & Kaplancıklı, Z. A. (2018). *Anticancer Agents Med. Chem.* **18**, 1606–1616.

Ardan, B., Kinzhybalo, V., Slyvka, Y., Shyyka, O., Luk'yanov, M., Lis, T. & Mys'kiv, M. (2017). *Acta Cryst.* C**73**, 36–46.

Berezin, A. S., Ivanova, A. D., Komarov, V. Y., Nadolinny, V. A. & Lavrenova, L. G. (2018). *New J. Chem.* **42**, 4902–4908.

Camí, G. E., Liu González, M., Sanz Ruiz, F. & Pedregosa, J. C. (2005). *J. Phys. Chem. Solids*, **66**, 936–945.

Chandra, S., Gautam, S., Rajor, H. K. & Bhatia, R. (2015). *Spectrochim. Acta A Mol. Biomol. Spectrosc.* **137**, 749–760.

Chen, C. J., Song, B. A., Yang, S., Xu, G. F., Bhadury, P. S., Jin, L. H., Hu, D. Y., Li, Q. Z., Liu, F., Xue, W., Lu, P. & Chen, Z. (2007). *Bioorg. Med. Chem.* **15**, 3981–3989.

Chen, J., Yi, C., Wang, S., Wu, S., Li, S., Hu, D. & Song, B. (2019). *Bioorg. Med. Chem. Lett.* **29**, 1203–1210.

Dolomanov, O. V., Bourhis, L. J., Gildea, R. J., Howard, J. A. K. & Puschmann, H. (2009). *J. Appl. Cryst.* **42**, 339–341.

Foroumadi, A., Soltani, F., Jabini, R., Moshafi, M. H. & Rasnani, F. M. (2004). *Arch. Pharm. Res.* **27**, 502–506.

Gowramma, B., Praveen, T. K., Gomathy, S., Kalirajan, R., Babu, B. & Krishnavenic, N. (2018). *Curr. Bioact. Compd.* **14**, 309–316.

Groom, C. R., Bruno, I. J., Lightfoot, M. P. & Ward, S. C. (2016). *Acta Cryst.* B**72**, 171–179.

Gurbanov, A. V., Mahmoudi, G., Guedes da Silva, M. F. C., Zubkov, F. I., Mahmudov, K. T. & Pombeiro, A. J. L. (2018). *Inorg. Chim. Acta*, **471**, 130–136.

Hangan, A. C., Turza, A., Stan, R. L., Stefan, R. & Oprean, L. S. (2015). *Russ. J. Coord. Chem.* **41**, 395–404.

Hassan, A. E., Shaaban, I. A., Abuelela, A. M., Zoghaib, W. M. & Mohamed, T. A. (2018). *J. Coord. Chem.* **71**, 2814–2830.

Huxel, T., Demeshko, S. & Klingele, J. (2015). *Z. Anorg. Allge Chem.* **641**, 1711–1717.

Ishankhodzhaeva, M. M., Kadyrova, S. A., Talipov, S. A., Ibragimov, B. T., Fun, K. K., Sundara Razh, S. S. & Parpiev, N. A. (2001). *Russ. J. Gen. Chem.* **71**, 1066–1069.

Ishankhodzhaeva, M. M., Umarov, B. B., Kadyrova, Sh. A., Parpiev, N. A., Makhkamov, K. K. & Talipov, S. A. (2000). *Russ. J. Gen. Chem.* **70**, 1113–1119.

Jakovljević, K., Matić, I. Z., Stanojković, T., Krivokuća, A., Marković, V., Joksović, M. D., Mihailović, N., Nićiforović, M. & Joksović, L. (2017). *Bioorg. Med. Chem. Lett.* **27**, 3709–3715.

Kadirova, Sh. A., Ishankhodzhaeva, M. M., Parpiev, N. A., Tozhiboev, A., Tashkhodzhaev, B. & Karimov, Z. (2008). *Russ. J. Gen. Chem.* **78**, 2398–2402.

Karaburun, A., Acar Çevik, U., Osmaniye, D., Sağlık, B., Kaya Çavuşoğlu, B., Levent, S. & Kaplancıklı, Z. (2018). *Molecules*, **23**, 3129. https://doi.org/10.3390/molecules23123129

Kaviarasan, L., Gowramma, B., Kalirajan, R., Mevithra, M. & Chandralekha, S. (2020). *J. Iran. Chem. Soc.* **17**, 2083–2094.

Kolavi, G., Hegde, V., Khazi, I. & Gadad, P. (2006). *Bioorg. Med. Chem.* **14**, 3069–3080.

Lavrenova, L. G., Sukhikh, T. S., Glinskaya, L. A., Trubina, S. V., Zvereva, V. V., Lavrov, A. N., Klyushova, L. S. & Artem'ev, A. V. (2023). *Int. J. Mol. Sci.* **24**, 13024.

Li, P., Shi, L., Yang, X., Yang, L., Chen, X. W., Wu, F., Shi, Q. C., Xu, W. M., He, M., Hu, D. Y. & Song, B. A. (2014). *Bioorg. Med. Chem. Lett.* **24**, 1677–1680.

Lynch, D. E. & Ewington, J. (2001). *Acta Cryst.* C**57**, 1032–1035.

Rigaku OD (2020). *CrysAlis PRO*. Rigaku Oxford Diffraction Ltd, Yarnton, England.

Sheldrick, G. M. (2015a). *Acta Cryst.* A**71**, 3–8.

Sheldrick, G. M. (2015b). *Acta Cryst.* C**71**, 3–8.

Slyvka, Y. (2017a). Visnyk Lviv Univ. Ser. Chem. **58**, 172.

Slyvka, Y., Kinzhybalo, V., Shyyka, O. & Mys'kiv, M. (2021). *Acta Cryst.* C**77**, 249–256.

Slyvka, Y. I. (2017b). *J. Struct. Chem.* **58**, 356–357.

Slyvka, Y. I., Goreshnik, E. A., Pokhodylo, N. T. & Mys'kiv, M. G. (2022). *J. Chem. Crystallogr.* **52**, 205–213.

Song, Y., Ji, Y.-F., Kang, M.-Y. & Liu, Z.-L. (2012). *Acta Cryst.* E**68**, m772.

Spackman, P. R., Turner, M. J., McKinnon, J. J., Wolff, S. K., Grimwood, D. J., Jayatilaka, D. & Spackman, M. A. (2021). *J. Appl. Cryst.* **54**, 1006–1011.

Swapna, M., Premakumari, C., Nagi Reddy, S., Padmaja, A. & Padmavathi, V. (2013). *Chem. Pharm. Bull.* **61**, 611–617.

Torambetov, B., Kadirova, S., Toshmurodov, T., Ashurov, J. M., Parpiev, N. A. & Ziyaev, A. (2019). *Acta Cryst.* E**75**, 1239–1242.

Toshmurodov, T. T., Ziyaev, A. A., Elmuradov, B. Zh., Ismailova, D. S. & Kurbanova, E. R. (2016). *J. Chem. Chem. Sci.* **6**, 199–204.

Upadhyay, P. K. & Mishra, P. (2017). *Rasayan J. Chem.* **10**, 254–262.

Wang, P., Wan, R., Wang, B., Han, F. & Wang, Y. (2009). *Acta Cryst.* E**65**, m1086.

Wang, T., Miao, W., Wu, S., Bing, G., Zhang, X., Qin, Z., Yu, H., Qin, X. & Fang, J. (2011). *Chin. J. Chem.* **29**, 959–967.

Yusuf, M., Khan, R. A. & Ahmed, B. (2008). *Bioorg. Med. Chem.* **16**, 8029–8034.

Synthesis, crystal structure and Hirshfeld surface analysis of bromidotetrakis-[5-(prop-2-en-1-ylsulfanyl)-1,3,4-thiadiazol-2-amine-*κN³*]copper(II) bromide

Aziz Atashov, Mukhlisakhon Azamova, Daminbek Ziyatov, Zamira Uzakbergenova, Batirbay Torambetov, Tamas Holczbauer, Jamshid Ashurov and Shakhnoza Kadirova

Computing details

Bromidotetrakis[5-(prop-2-en-1-ylsulfanyl)-1,3,4-thiadiazol-2-amine-*κN³*]copper(II) bromide

Crystal data

$[CuBr(C_5H_7N_3S_2)_4]Br$	$D_x = 1.663$ Mg m^{-3}
$M_r = 916.38$	Cu $K\alpha$ radiation, $\lambda = 1.54184$ Å
Tetragonal, $P4/n$	Cell parameters from 9121 reflections
$a = 12.69368$ (9) Å	$\theta = 3.5$–70.8°
$c = 11.35879$ (13) Å	$\mu = 7.95$ mm^{-1}
$V = 1830.24$ (3) Å^3	$T = 293$ K
$Z = 2$	Block, green
$F(000) = 918$	$0.12 \times 0.08 \times 0.03$ mm

Data collection

XtaLAB Synergy, Single source at home/near, HyPix3000 diffractometer	18450 measured reflections
	1746 independent reflections
Detector resolution: 10.0000 pixels mm^{-1}	1597 reflections with $I > 2\sigma(I)$
ω scans	$R_{int} = 0.036$
Absorption correction: multi-scan (CrysAlisPro; Rigaku OD, 2020)	$\theta_{max} = 69.9°$, $\theta_{min} = 3.9°$
	$h = -15 \rightarrow 15$
	$k = -11 \rightarrow 15$
$T_{min} = 0.626$, $T_{max} = 1.000$	$l = -13 \rightarrow 13$

Refinement

Refinement on F^2	H-atom parameters constrained
Least-squares matrix: full	$w = 1/[\sigma^2(F_o^2) + (0.0273P)^2 + 0.9257P]$ where $P = (F_o^2 + 2F_c^2)/3$
$R[F^2 > 2\sigma(F^2)] = 0.025$	
$wR(F^2) = 0.065$	$(\Delta/\sigma)_{max} < 0.001$
$S = 1.05$	$\Delta\rho_{max} = 0.26$ e Å^{-3}
1746 reflections	$\Delta\rho_{min} = -0.28$ e Å^{-3}
118 parameters	Extinction correction: SHELXL-2016/6 (Sheldrick 2015b), $Fc^* = kFc[1+0.001xFc^2\lambda^3/\sin(2\theta)]^{-1/4}$
0 restraints	
Hydrogen site location: inferred from neighbouring sites	Extinction coefficient: 0.00018 (7)

Special details

Geometry. All esds (except the esd in the dihedral angle between two l.s. planes) are estimated using the full covariance matrix. The cell esds are taken into account individually in the estimation of esds in distances, angles and torsion angles; correlations between esds in cell parameters are only used when they are defined by crystal symmetry. An approximate (isotropic) treatment of cell esds is used for estimating esds involving l.s. planes.

Fractional atomic coordinates and isotropic or equivalent isotropic displacement parameters (Å²)

	x	*y*	*z*	$U_{iso}*/U_{eq}$	Occ. (<1)
Br1	0.750000	0.750000	1.01564 (4)	0.04943 (15)	
Br2	0.250000	0.750000	1.000000	0.05616 (16)	
Cu1	0.750000	0.750000	0.77377 (5)	0.03890 (16)	
S1	0.39660 (5)	0.70986 (6)	0.72047 (6)	0.06176 (19)	
S2	0.42895 (6)	0.65094 (8)	0.46657 (7)	0.0831 (3)	
N2	0.59625 (14)	0.71817 (14)	0.74447 (16)	0.0470 (4)	
N1	0.57992 (14)	0.68882 (16)	0.62785 (18)	0.0544 (5)	
N3	0.50405 (16)	0.7637 (2)	0.9157 (2)	0.0739 (7)	
H3A	0.560992	0.775718	0.954484	0.089*	
H3B	0.443808	0.771729	0.949189	0.089*	
C1	0.50915 (16)	0.73279 (18)	0.8039 (2)	0.0500 (5)	
C2	0.48136 (19)	0.6828 (2)	0.6037 (2)	0.0574 (6)	
C3	0.5494 (3)	0.6360 (3)	0.3816 (3)	0.0984 (11)	
H3BC	0.580640	0.704195	0.365145	0.118*	0.5
H3BD	0.600153	0.593336	0.423967	0.118*	0.5
H3AA	0.600532	0.688177	0.406669	0.118*	0.5
H3AB	0.579095	0.566715	0.395347	0.118*	0.5
C5A	0.5337 (16)	0.5753 (12)	0.1730 (17)	0.143 (7)	0.5
H5AA	0.587593	0.612982	0.136912	0.171*	0.5
H5AB	0.492013	0.529830	0.128742	0.171*	0.5
C4	0.5259 (9)	0.6502 (7)	0.2475 (9)	0.104 (3)	0.5
H4	0.516751	0.720330	0.226229	0.125*	0.5
C4A	0.5181 (8)	0.5852 (11)	0.2749 (8)	0.112 (3)	0.5
H4A	0.461720	0.541488	0.293578	0.134*	0.5
C5	0.5187 (14)	0.6021 (18)	0.1813 (12)	0.154 (8)	0.5
H5A	0.526312	0.529967	0.192763	0.185*	0.5
H5B	0.504113	0.628295	0.106619	0.185*	0.5

Atomic displacement parameters (Å²)

	U^{11}	U^{22}	U^{33}	U^{12}	U^{13}	U^{23}
Br1	0.05153 (19)	0.05153 (19)	0.0452 (3)	0.000	0.000	0.000
Br2	0.04993 (19)	0.04993 (19)	0.0686 (3)	0.000	0.000	0.000
Cu1	0.0362 (2)	0.0362 (2)	0.0443 (3)	0.000	0.000	0.000
S1	0.0387 (3)	0.0791 (4)	0.0675 (4)	0.0015 (3)	−0.0065 (3)	0.0060 (3)
S2	0.0637 (4)	0.1138 (7)	0.0718 (5)	−0.0029 (4)	−0.0179 (4)	−0.0189 (4)
N2	0.0405 (9)	0.0489 (10)	0.0517 (10)	−0.0013 (8)	−0.0029 (8)	0.0008 (8)
N1	0.0450 (10)	0.0610 (12)	0.0573 (11)	−0.0041 (9)	−0.0020 (8)	−0.0070 (9)
N3	0.0430 (11)	0.121 (2)	0.0573 (13)	0.0096 (12)	0.0002 (9)	−0.0060 (13)

C1	0.0388 (11)	0.0538 (12)	0.0574 (13)	0.0016 (9)	−0.0018 (9)	0.0079 (10)
C2	0.0489 (13)	0.0608 (14)	0.0626 (15)	−0.0020 (11)	−0.0058 (11)	−0.0008 (11)
C3	0.084 (2)	0.131 (3)	0.080 (2)	−0.004 (2)	−0.0020 (18)	−0.023 (2)
C5A	0.168 (13)	0.095 (7)	0.165 (16)	−0.031 (7)	0.075 (10)	−0.020 (7)
C4	0.173 (9)	0.068 (5)	0.070 (6)	−0.034 (5)	0.017 (5)	0.007 (4)
C4A	0.117 (7)	0.141 (10)	0.077 (6)	0.013 (7)	0.024 (5)	−0.019 (6)
C5	0.121 (9)	0.30 (2)	0.038 (4)	0.016 (12)	−0.010 (5)	−0.005 (8)

Geometric parameters (Å, º)

Br1—Cu1	2.7474 (7)	C3—H3BC	0.9700
Cu1—N2^i	2.0206 (17)	C3—H3BD	0.9700
Cu1—N2	2.0206 (17)	C3—H3AA	0.9700
Cu1—N2^{ii}	2.0206 (17)	C3—H3AB	0.9700
Cu1—N2^{iii}	2.0206 (17)	C3—C4	1.562 (11)
S1—C1	1.739 (2)	C3—C4A	1.429 (10)
S1—C2	1.742 (3)	C5A—H5AA	0.9300
S2—C2	1.741 (3)	C5A—H5AB	0.9300
S2—C3	1.818 (4)	C5A—C4A	1.181 (19)
N2—N1	1.392 (3)	C4—H4	0.9300
N2—C1	1.308 (3)	C4—C5	0.973 (18)
N1—C2	1.283 (3)	C4A—H4A	0.9300
N3—H3A	0.8600	C5—H5A	0.9300
N3—H3B	0.8600	C5—H5B	0.9300
N3—C1	1.331 (3)		
N2^i—Cu1—Br1	99.48 (5)	S2—C3—H3BC	110.7
N2^{iii}—Cu1—Br1	99.48 (5)	S2—C3—H3BD	110.7
N2^{ii}—Cu1—Br1	99.48 (5)	S2—C3—H3AA	109.6
N2—Cu1—Br1	99.48 (5)	S2—C3—H3AB	109.6
N2^{ii}—Cu1—N2^{iii}	88.446 (18)	H3BC—C3—H3BD	108.8
N2^{ii}—Cu1—N2	88.446 (18)	H3AA—C3—H3AB	108.1
N2^{iii}—Cu1—N2^i	88.446 (18)	C4—C3—S2	110.2 (5)
N2^i—Cu1—N2	88.445 (18)	C4—C3—H3AA	109.6
N2^{ii}—Cu1—N2^i	161.04 (11)	C4—C3—H3AB	109.6
N2^{iii}—Cu1—N2	161.04 (11)	C4A—C3—S2	105.3 (5)
C1—S1—C2	86.58 (11)	C4A—C3—H3BC	110.7
C2—S2—C3	100.25 (14)	C4A—C3—H3BD	110.7
N1—N2—Cu1	110.74 (13)	H5AA—C5A—H5AB	120.0
C1—N2—Cu1	134.66 (16)	C4A—C5A—H5AA	120.0
C1—N2—N1	113.76 (18)	C4A—C5A—H5AB	120.0
C2—N1—N2	111.4 (2)	C3—C4—H4	112.8
H3A—N3—H3B	120.0	C5—C4—C3	134.4 (15)
C1—N3—H3A	120.0	C5—C4—H4	112.8
C1—N3—H3B	120.0	C3—C4A—H4A	106.8
N2—C1—S1	112.94 (18)	C5A—C4A—C3	146.4 (13)
N2—C1—N3	125.1 (2)	C5A—C4A—H4A	106.8
N3—C1—S1	121.96 (17)	C4—C5—H5A	120.0

S2—C2—S1	119.40 (14)	C4—C5—H5B	120.0
N1—C2—S1	115.33 (19)	H5A—C5—H5B	120.0
N1—C2—S2	125.3 (2)		
Cu1—N2—N1—C2	−170.89 (17)	C1—S1—C2—S2	−178.55 (17)
Cu1—N2—C1—S1	168.95 (12)	C1—S1—C2—N1	1.2 (2)
Cu1—N2—C1—N3	−9.9 (4)	C1—N2—N1—C2	0.2 (3)
S2—C3—C4—C5	−103 (2)	C2—S1—C1—N2	−1.01 (18)
S2—C3—C4A—C5A	148 (2)	C2—S1—C1—N3	177.9 (2)
N2—N1—C2—S1	−1.0 (3)	C2—S2—C3—C4	−158.1 (4)
N2—N1—C2—S2	178.68 (17)	C2—S2—C3—C4A	166.4 (6)
N1—N2—C1—S1	0.7 (2)	C3—S2—C2—S1	178.11 (19)
N1—N2—C1—N3	−178.2 (2)	C3—S2—C2—N1	−1.6 (3)

Symmetry codes: (i) y, $-x+3/2$, z; (ii) $-y+3/2$, x, z; (iii) $-x+3/2$, $-y+3/2$, z.

Hydrogen-bond geometry (Å, º)

D—H···A	D—H	H···A	D···A	D—H···A
N3—H3A···Br1	0.86	2.52	3.3265 (1)	157
N3—H3B···Br2	0.86	2.54	3.3685 (1)	162
C5A—H5AA···Br1[iv]	0.93	3.03	3.95 (2)	175

Symmetry code: (iv) x, y, $z-1$.